

Same sign top-pairs in a non-universal Z' model at the LHC

Sudhir Kumar Gupta*

Dept of Physics & Astronomy, Iowa State University, Ames, IA 50011.

(Dated: November 24, 2010)

Abstract

We analyse same sign dilepton signatures in a non-universal flavor changing Z' model. These arise due to $t\bar{t}$ (or $t\bar{t}$) production processes due to the semi-leptonic decays of (anti)tops. We also discuss top reconstruction and spin measurement using the variable M_{T_2} and M_{T_2} -Assisted On-Shell (MAOS) Momentum techniques and will also provide a comparison with the on-shell mass relation method. Sensitivities to the flavor-changing top coupling has also been estimated for different LHC energies and projected LHC luminosities corresponding to them.

*Electronic address: skgupta@iastate.edu

I. INTRODUCTION

Presence of extra Z' bosons is dictated by a wide range of extensions to the Standard Model (SM). These arise due to presence of additional abelian gauge symmetries $U(1)$, as part of extended SM gauge groups $G_{SM} \times U(1)^N$; $N=1,2,\dots$ [1]. Phenomenology of such models is interesting as these couples to the SM fermions with flavor-diagonal as well as off-diagonal couplings. A Z' which couples to SM fermions with flavor violating couplings is even interesting as it, besides contributing to large top-quark forward-backward asymmetry $A_{FB}^t = .193 \pm .069$, as measured at the Tevatron, tree-level quark sector Flavor-changing neutral currents (FCNCs) [2] which were suppressed in the SM, also give rise to interesting collider signatures such as same sign top pairs, associated production of Z' with a top or antitop[3].

In traditional Z' model, flavor violating coupling to the quarks are tiny so the process $t\bar{t}$ is irrelevant in those cases. However it has been recently argued in the Refs. [4], [5] that at least some of these flavor off-diagonal couplings can be comparable to V_{tb} in models where a right chiral Z' couples in a non-trivial way to the up-quarks.

The aim of this paper is to study in detail the like sign signatures in the context of the Large Hadron Collider (LHC) which arise via the same sign top pair production. This is interesting as it will serve as a direct probe to the nature of Z' and its coupling to the quarks.

Organisation of the article is as follows: In the next Section we will briefly discuss about the model and its experimental constraints. In Section 3, we will discuss the top and anti-top pair production cross-section for a wide range of Z' mass. We will work with same sign dilepton signature at the LHC, top reconstruction, and spin measurement of Z' in Section 4. We will also discuss LHC sensitivities to the model in the same Section. Finally we will summarise our findings in Section 5.

II. THE MODEL

As has been discussed in the previous section, in our model, the new vector boson Z' couples with the up quarks via the right handed coupling with the following interaction terms

$$\mathcal{L} \ni G_{ij} Z'_\mu \bar{Q}_{iL} \gamma^\mu P_R u_{jR} + h.c. \quad (1)$$

where G_{ij} is a 3×3 matrix of the form

$$\begin{pmatrix} 0 & 0 & \eta_{13} \\ 0 & 0 & \eta_{23} \\ \eta_{31} & \eta_{32} & 0 \end{pmatrix}$$

It has been pointed out by the authors of Ref. [5], that the couplings η_{31} , η_{32} can be $\sim V_{tb} \gg \eta_{33} \sim V_{td,s}$ which is consistent with the low energy flavor data

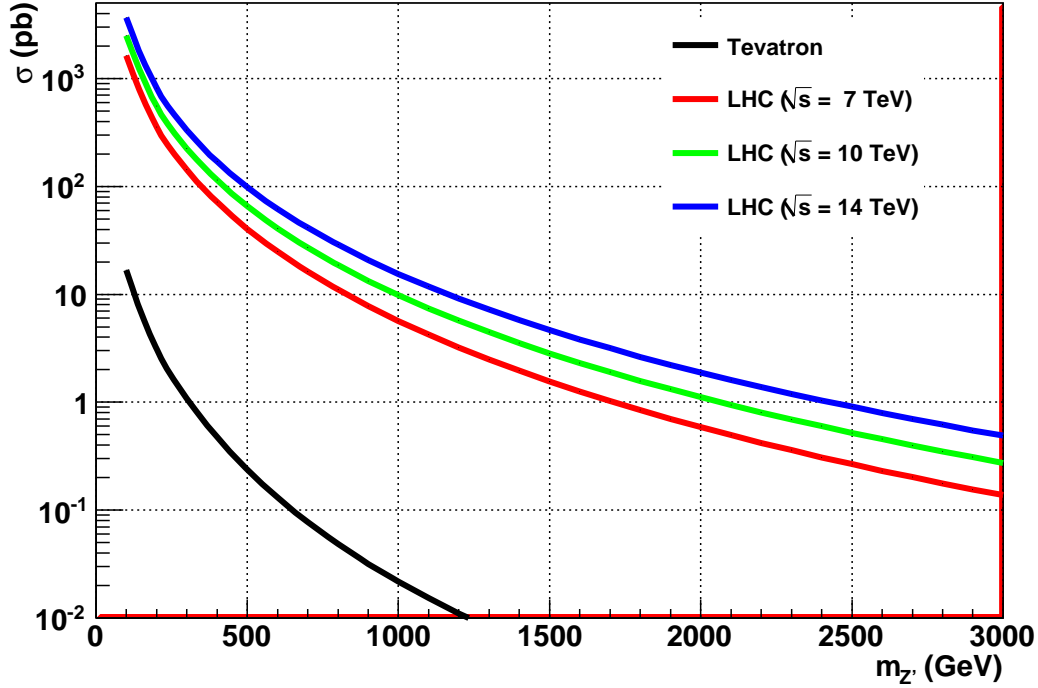


FIG. 1: Tevatron and LHC cross-sections for same-sign top pair productions at the Tevatron and LHC with \sqrt{s} as 1.98 (Black), 7 (Red), 10 (Green) and 14 TeV (Blue) respectively. $g_X = 1$ is assumed here.

such as meson mixing and $K - decays$ [6]. It has also been discussed in the same article that the model will be free from any such constraints provided only one flavor violating coupling is non-zero. In our study we will not restrict ourselves with the aforementioned coupling to be $\sim \mathcal{O}(1)$, but will rather study a whole range with $\eta_{31} \neq 0$. Thus, the relevant interaction term will take the following form

$$\mathcal{L} \ni g_X Z'_\mu \bar{u} \gamma^\mu P_R t + h.c. \quad (2)$$

with $g_X \in (0, 1]$.

III. (SAME-SIGN) TOP PAIR PRODUCTION

If the flavor violating coupling $u - t - Z'$ is sufficiently large, we expect to observe plenty of same sign top pairs at the LHC depending upon its coupling. With the setup we have, the only responsible subprocesses for the same sign (anti)top pairs are $\bar{u}\bar{u} \rightarrow \bar{t}\bar{t}$ and $uu \rightarrow tt$. These occurs by the t- (and u-) channel exchange of the Z' .

We present total cross-section for the processes $tt + \bar{t}\bar{t}$ at the LHC and the Tevatron for a wide range of Z' mass between 0.1 – 3 TeV in Fig. 1. We use

CTEQ6L1 to estimate the parton densities in our cross-section calculation. The two QCD scales, i.e. the renormalization scale, μ_R , and the factorization scale μ_F are fixed at

$$\mu_R = \sqrt{\hat{s}} = \mu_F. \quad (3)$$

We do not use the K-factors in our cross-section calculation. If these are similar to as given in the Ref. [7], the rates are expected to go up by about $\sim 20\%$ at *NNLO-NLL*.

It is worth to note here that, at the Tevatron the contribution to the total cross-section due to $t\bar{t}$ and $t\bar{t}$ are the same, i.e. $R_t = \sigma_{t\bar{t}}/\sigma_{t\bar{t}} = 1$. This is because, at the Tevatron, in both production processes one parton is always a valence up-quark while the other is a sea up-quarks. However at the LHC the situation is quite different, i.e. in one case ($t\bar{t}$) both the partons are either valence quarks while in other $t\bar{t}$ these are sea quarks. Clearly, we expect, R_t to be < 1 at the LHC. (See Figure 2)

A couple of interesting remarks about these ratios: (a) R_t 's are independent of the coupling constant, and, also (b) independent of higher order QCD and electroweak correction as these corrections will be exactly same for both $\bar{u}\bar{u} \rightarrow t\bar{t}$ and $uu \rightarrow t\bar{t}$, thus cancel between the denominator and the numerator. Another interesting feature about these ratios is that these will remain intact for a similar detection mode due to cancelation of branching ratios between tops and antitops.

Clearly such ratios can serve as an important tool to probe $m_{Z'}$ in addition to other kinematic variables.

IV. SAME SIGN DILEPTONS AT THE LHC

With their cross-sections given as in Figure 1, *a priori*, we will have enough events well above the Tevatron reach of same sign top pairs with $g_X \sim 0.01$ for $m_{Z'} = 300$ GeV and $g_X \sim 0.2$ for $m_{Z'} = 1.2$ TeV respectively, in case both tops are fully reconstructed in all their decay modes.

Semileptonic decays of the produced tops give rise to a very striking form of LHC signature in the form of a pair of same sign leptons accompanied by a pair of b-jets and some missing energy, \cancel{E}_T due to missing neutrinos from the decay of each top. These same sign dileptons are expected to serve as a remarkable probe to the new physics models where the decay chain of pair produced new resonances can lead to dileptons [8]. In our study also, this is a unique signature to the same sign (anti-)top pairs with almost negligible SM background.

For our analysis, we generated top pair events using **MadGraph** [9–11]. we produced MadGraph model files that incorporates the new particle Z' and the FCNC

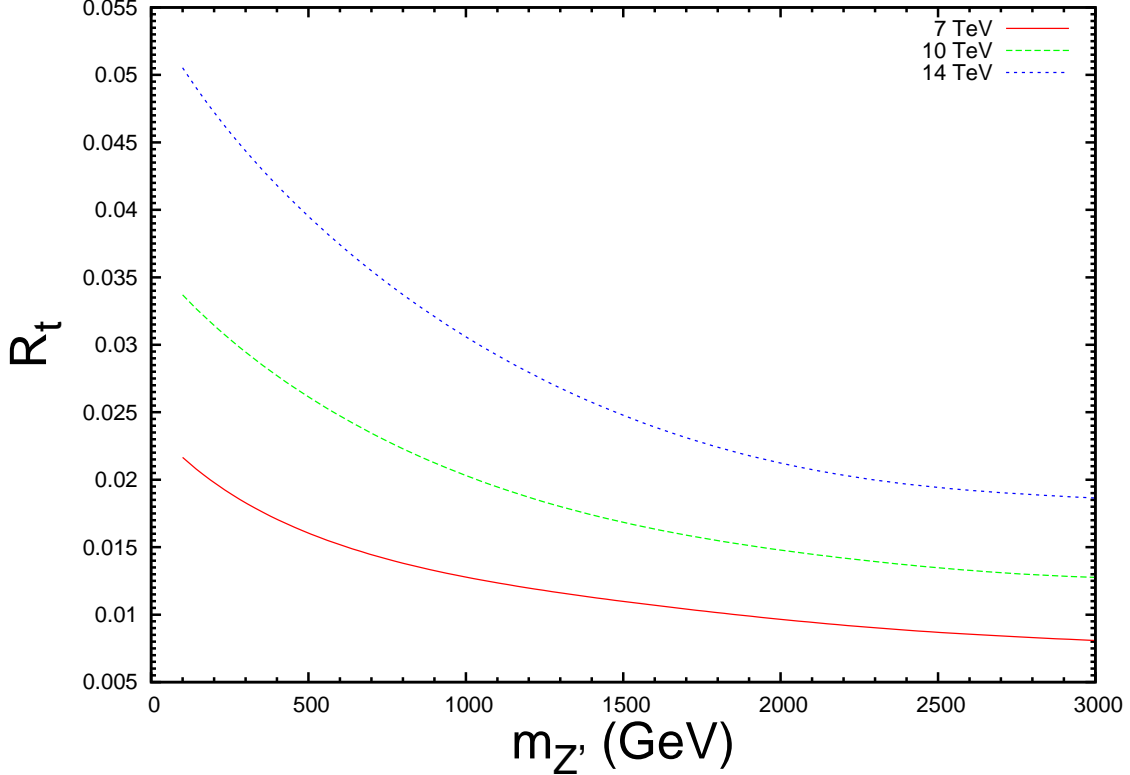


FIG. 2: Ratio $R_t = \sigma_{t\bar{t}}/\sigma_{tt}$ vs $m_{Z'}$ at the LHC for $\sqrt{S} = 7, 10$ and 14 TeV. Color convention is the same as in Figure 1.

couplings of Eq. 1 into MadGraph ¹.

In order to study the process, $pp \rightarrow l^\pm l^\pm + bb + \cancel{E}_T$, we choose $m_{Z'} = .5, 1$ and 1.5 TeV. The coupling g_x is fixed at unity so that for a given g_x , the event rates can be easily obtained simply by multiplying the factor g_x^4 . We present our results for the present LHC centre-of-mass (CM) energy, $\sqrt{S} = 7$ TeV as well as for 10 TeV and 14 TeV.

The event analysis is performed with PYTHIA [12] at the parton level, turning off initial- and final-state radiation. To select our same sign dilepton (SSD) states, we impose the following minimal acceptance cuts on our event samples:

- Both lepton should have $p_{T_l} > 25$ GeV and $|\eta_l| \leq 2.7$, to ensure that they lie within the coverage of the detector.
- b-jets should have $p_{T_b} > 25$ GeV and $|\eta_b| \leq 2.5$
- Spatial resolution between *lepton - lepton*, *lepton - b-jet*, and, *b-jet - b-jet* should be $\Delta R_{ll} \geq 0.4$, $\Delta R_{lb} \geq 0.4$, $\Delta R_{bb} \geq 0.4$ respectively, (where $\Delta R_{ij} = \sqrt{\Delta\eta_{ij}^2 + \Delta\phi_{ij}^2}$, $\Delta\eta_{ij} = \eta_i - \eta_j$, $\Delta\phi_{ij} = \phi_i - \phi_j$), such that the leptons are well separated in space.

¹ These modifications are available upon request.

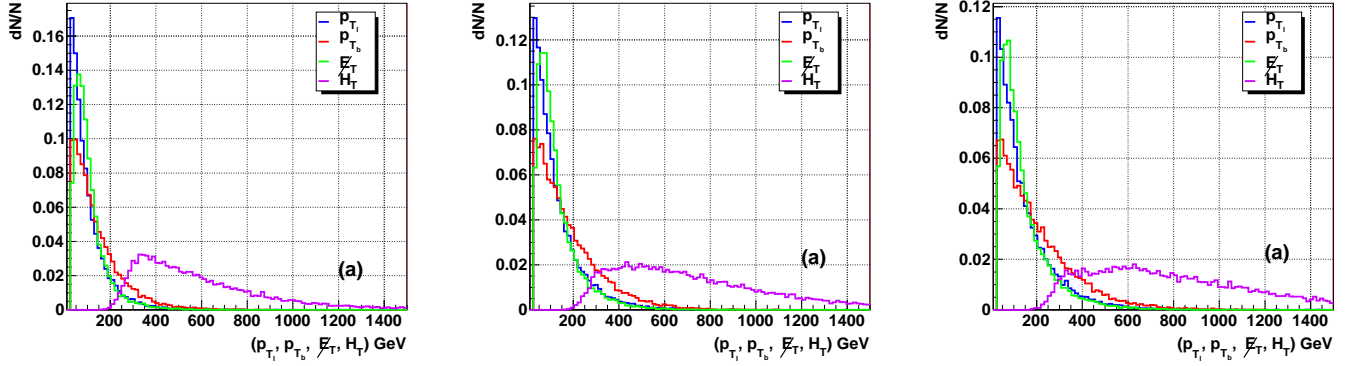


FIG. 3: Differential distributions for lepton and b-jet- p_T ($p_{T_{l,b}}$), missing energy \cancel{E}_T , and scalar- p_T (H_T). $m_{Z'} = 0.5, 1$ and 1.5 TeV in Figures (a), (b) and (c) respectively. $\sqrt{S} = 7$ TeV is assumed here.

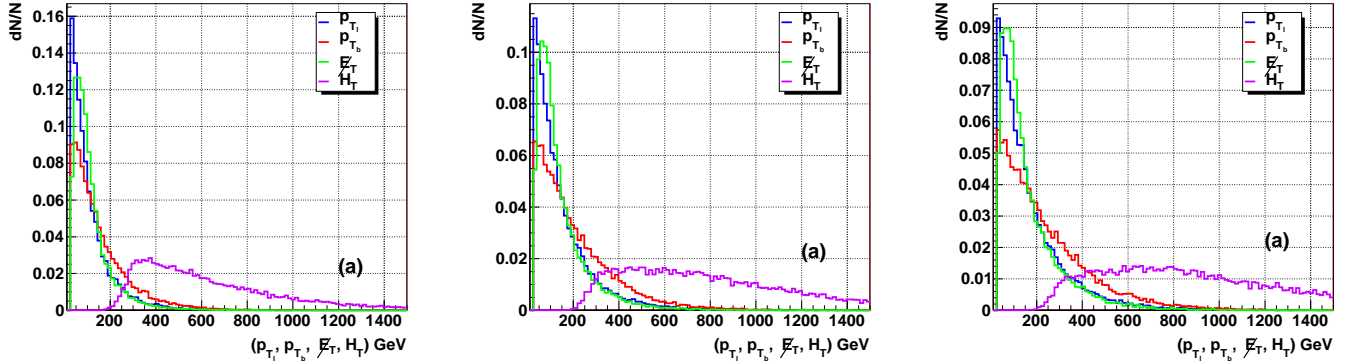


FIG. 4: Differential distributions for lepton and b-jet- p_T ($p_{T_{l,b}}$), missing energy \cancel{E}_T , and scalar- p_T (H_T). $m_{Z'} = 0.5, 1$ and 1.5 TeV in Figures (a), (b) and (c) respectively. $\sqrt{S} = 10$ TeV is assumed here.

- A missing transverse energy cut, $\cancel{E}_T > 30$ GeV to ensure that leptons are due to W decay.

In our event analysis we also allow leptonic decays of τ^\pm 's into e^\pm or μ^\pm . Though the lepton arising from the τ decays are relatively softer, yet they can contribute by $\sim 3\%$ in the total event rates. Finally, we also used the b-tagging efficiency ~ 58 percent as expected in the ATLAS and CMS experiments [13].

We present kinematical distributions for lepton and b-jet transverse momentum, missing energy and the scalar sum of p_T 's of all the visible final state particles and the missing transverse energy, i.e.

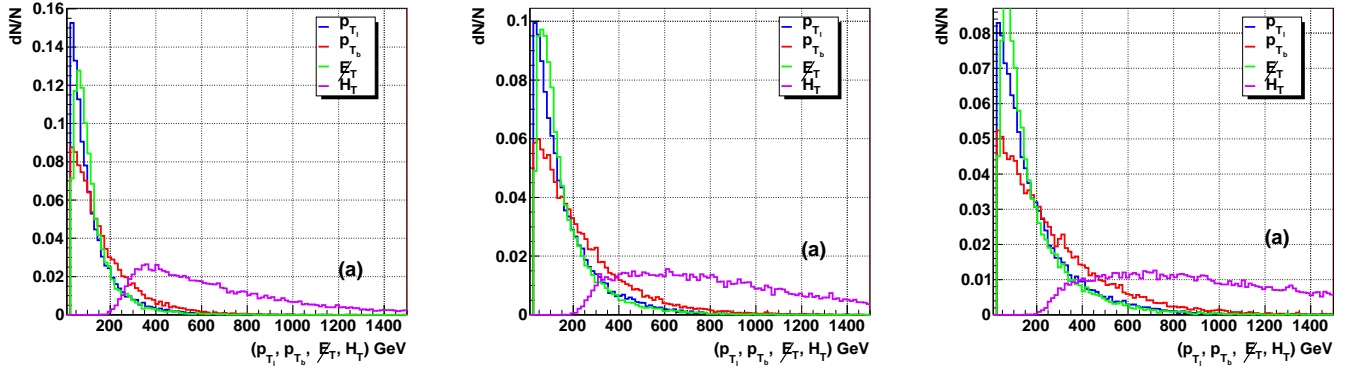


FIG. 5: Differential distributions for lepton and b-jet- p_T ($p_{T_{l,b}}$), missing energy \cancel{E}_T , and scalar- p_T (H_T). $m_{Z'} = 0.5, 1$ and 1.5 TeV in Figures (a), (b) and (c) respectively. $\sqrt{S} = 14$ TeV is assumed here.

$$H_T = p_{T_{vis}} + \cancel{E}_T = \sum_{l,b} p_T + |\mathbf{p}_T| = \sum_{l,b} p_T + \left| -\sum_{l,b} \mathbf{p}_T \right| \quad (4)$$

for different LHC energies in Figs. 3-5 at the LHC for $\sqrt{S} = 7, 10$, and, 14 TeV for three different values of Z' mass in each case as $0.5, 1$ and 1.5 TeV. We normalised our distribution with the total number of events in each case. Though finally it is irrelevant what value of g_x we choose in these normalised distributions as the factor g_x^2 will cancel between the numerator and the denominator, we use $g_x = 1$ in our simulation.

Keeping in mind about future LHC runs with different amount of data, we present SSD event rates in Table I for both the processes $l^-l^- + \bar{b}b + \cancel{E}_T$ and $l^+l^+ + bb + \cancel{E}_T$ as well as the sum of the two. It is to be noted that once including the available K-factor at NNLO-NLL, our predictions for the event rate will go up by a factor of 1.2.

With the events with the aforementioned kinematical distribution, our next task is to confirm whether such signatures are really due to the top-pair production. Also, once the top are reconstructed the next level question to ask is about the nature of the exchanged particle. Keeping this in mind, In the remaining part of the

\sqrt{S} (TeV), $\int \mathcal{L} dt$ (fb $^{-1}$)	$m_{Z'} = 0.5$ TeV	$m_{Z'} = 1$ TeV	$m_{Z'} = 1.5$ TeV
7, 0.1	27 (0, 27)	4 (0, 4)	1 (0, 1)
10, 0.5	221 (5, 216)	40 (1, 39)	12 (0, 12)
14, 10	6690 (252, 6438)	1268 (36, 1232)	397 (9, 388)

TABLE I: Number of SSD events at the LHC for $m_{Z'} = 0.5, 1$ and 1.5 TeV at the LHC for \sqrt{S} as 7, 10 and 14 TeV. $g_x = 1$ is assumed in this table. Also shown are the number of events with $l^-l^- + \bar{b}b + \cancel{E}_T$ and $l^+l^+ + bb + \cancel{E}_T$ events respectively, inside the brackets.

section we will deal with issues such as top pair reconstruction, which is analogous to reconstructing four-momenta of the missing neutrino pair. Later use the information to reconstruct complete subprocess in order to probe the mass and spin information of the exchanged Z' . Let us begin with the top mass reconstruction in the next subsection.

A. Top Reconstruction

Since in these final states, the missing transverse energy is mostly composed of two invisible neutrinos, it is not obvious to reconstruct tops. Yet, due to the fact the produced particles and their decay chains are identical, it is still possible to reconstruct them fully up to a finite degree of accuracy through the following two methods. These are: (a) Mass relation method (MRM), and, (b) M_{T_2} -Assisted On-Shell Momentum (MAOS) method. Below we discuss them one by one in detail in the present context:

1. Mass relation Method

In this method we use the known on-shell mass relations involving four-momenta of various final state particles and make use of the two missing transverse momentum relations. Thus, we have

$$p_{\nu_1}^2 = 0 \tag{5a}$$

$$p_{\nu_2}^2 = 0 \tag{5b}$$

$$(p_{l_1} + p_{\nu_1})^2 = m_W^2 \tag{5c}$$

$$(p_{l_2} + p_{\nu_2})^2 = m_W^2 \tag{5d}$$

$$(p_{l_1} + p_{b_1} + p_{\nu_1})^2 = m_t^2 \tag{5e}$$

$$(p_{l_2} + p_{b_2} + p_{\nu_2})^2 = m_t^2 \tag{5f}$$

$$\mathbf{p}_{T_{\nu_1}} + \mathbf{p}_{T_{\nu_2}} = \mathbf{\not{p}}_T = - \sum_{l,b} \mathbf{p}_T \tag{5g}$$

2. M_{T_2} -Assisted On-Shell Momentum (MAOS) Technique

Though, as we will see later that the previous method works fine, yet it has a major drawback, i.e. we need to use mass of the top explicitly in the aforementioned mass relations. Recently a new method, call MT2-method [14] has been found to overcome this problem. This method uses the mass-relations in a slightly different way to first define the variable m_{T_2} as

$$M_{T_2}(m_{\mathcal{U}}) = \min_{\mathbf{p}_T^{(1)}, \mathbf{p}_T^{(2)}} \left[\max \left\{ M_T \left(m_{\mathcal{U}}; \mathbf{p}_T^{(1)} \right), M_T \left(m_{\mathcal{U}}; \mathbf{p}_T^{(2)} \right) \right\} \right], \quad (6)$$

where M_T , the transverse mass of each parent particle, is defined as

$$M_T(m_{\mathcal{U}}; \mathbf{p}_T^{\mathcal{U}}) = \sqrt{m_{\mathcal{V}}^2 + m_{\mathcal{U}}^2 + 2(E_T^{\mathcal{V}} E_T^{\mathcal{U}} - \mathbf{p}_T^{\mathcal{V}} \cdot \mathbf{p}_T^{\mathcal{U}})}. \quad (7)$$

Here \mathcal{U} and \mathcal{V} represent the individual undetected (invisible) and detected (visible) particles, respectively, $\mathbf{p}_T^{(1)}$ and $\mathbf{p}_T^{(2)}$ are transverse momenta of two invisible particles and $m_{\mathcal{U}}$ is the mass of the invisible particle. The minimization is performed with the constraint $\mathbf{p}_T^{(1)} + \mathbf{p}_T^{(2)} = \not{p}_T$.

One interesting thing about this method is that mass of the top is determined before the determination of longitudinal momentum of the invisible neutrinos which is due to the fact that we are dealing with transverse masses.

Now, once we obtained transverse momenta of the missing neutrinos through the aforementioned way as, $\mathbf{p}_T^{\mathcal{U}_i} = \mathbf{p}_T^{(i)}$, we can obtain the longitudinal components by solving,

$$p_L^{\mathcal{U}} = \frac{1}{(E_T^{\mathcal{V}})^2} \left[\mathcal{A} p_L^{\mathcal{V}} \pm \sqrt{(p_L^{\mathcal{V}})^2 + (E_T^{\mathcal{V}})^2} \sqrt{\mathcal{A}^2 - (E_T^{\mathcal{V}} E_T^{\mathcal{U}})^2} \right] \quad (8)$$

where

$E_T^{\mathcal{V}} = \sqrt{(p^{\mathcal{V}})^2 + |\mathbf{p}_T^{\mathcal{V}}|^2}$, $E_T^{\mathcal{U}} = \sqrt{(p^{\mathcal{U}})^2 + |\mathbf{p}_T^{\mathcal{U}}|^2}$, and $\mathcal{A} = \frac{1}{2} \{m_{\mathcal{P}}^2 - m_{\mathcal{U}}^2 - (p^{\mathcal{V}})^2\} + \mathbf{p}_T^{\mathcal{V}} \cdot \mathbf{p}_T^{\mathcal{U}}$. $m_{\mathcal{P}}$, $m_{\mathcal{U}}$ are the masses of produced particle and the invisible particle respectively.

In our case the top mass and the unknown neutrino momenta are obtained by setting, $\mathcal{P} = t$, $\mathcal{U} = \nu$ and $\mathcal{V} = b + l$ in the aforementioned equations 6-8.

We present reconstructed top mass in Figs. 6-8 using both the methods. It is clear that the M_{T_2} method does a little better job which is due to the fact it requires lesser information than the mass relation method. But at practical level, these hardly differ for the process under consideration, though, of course, the former is very helpful specially in longer decay chains such as in supersymmetry, universal extra dimensions and little Higgs models.

B. Z' Spin Measurement

With the reconstructed momenta as obtained in the previous section, and hence the $\sqrt{\hat{s}}$, we can fully reconstruct the partonic process just like a e^+e^- collider. To gain more insight of the process, we investigate the angular distribution of the top in the parton CM frame. Results are presented in Figs 9. We note that dip gets smaller with the rising Z' mass, which will hint towards Z' mass in addition to confirming vector nature of the exchange particle. As has been established in Ref. [15] that

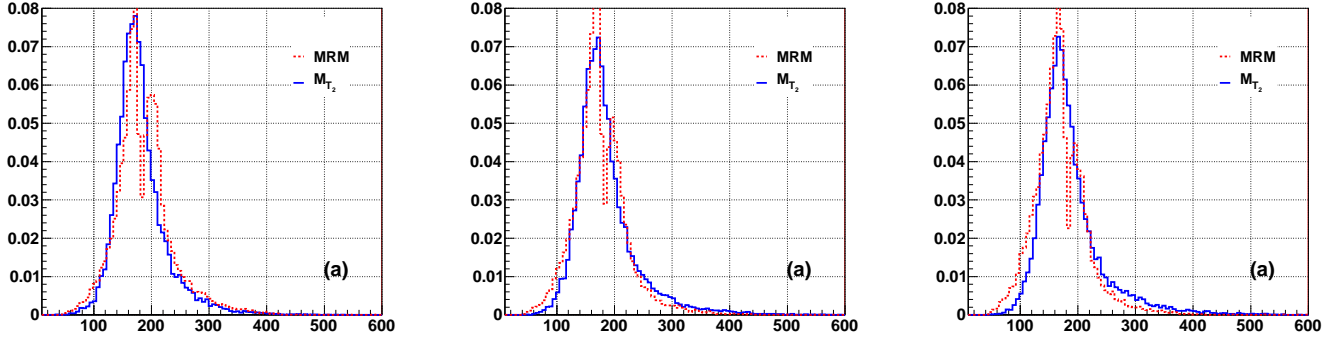


FIG. 6: Reconstructed top mass using the variable m_{T_2} for the event samples with $m_{Z'} = 0.5, 1$ and 1.5 TeV in Figures (a), (b) and (c) respectively. $\sqrt{S} = 7$ TeV is assumed here.

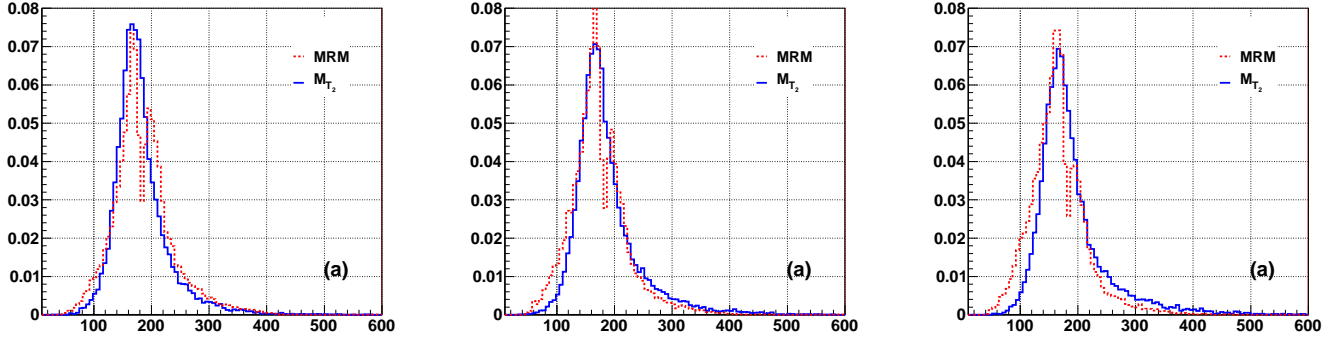


FIG. 7: Reconstructed top mass using the variable m_{T_2} for the event samples with $m_{Z'} = 0.5, 1$ and 1.5 TeV in Figures (a), (b) and (c) respectively. $\sqrt{S} = 10$ TeV is assumed here.

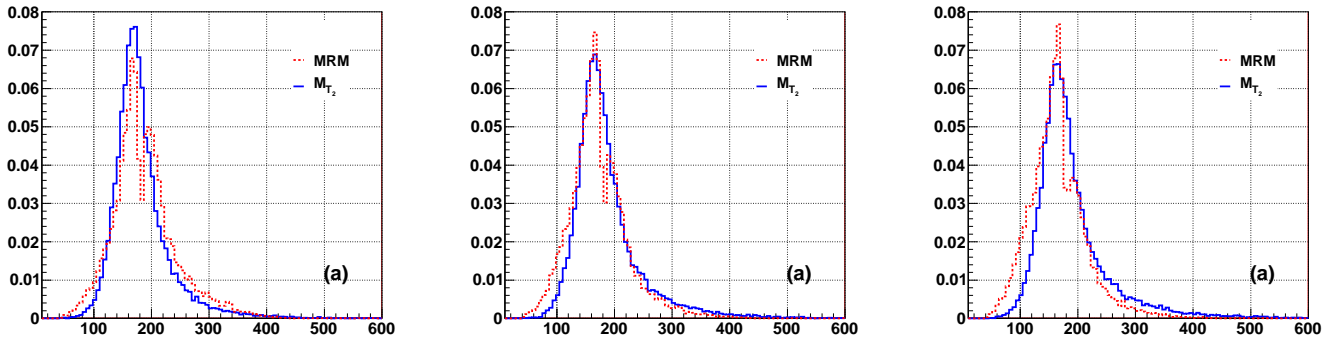


FIG. 8: Reconstructed top mass using the variable m_{T_2} for the event samples with $m_{Z'} = 0.5, 1$ and 1.5 TeV in Figures (a), (b) and (c) respectively. $\sqrt{S} = 14$ TeV is assumed here.

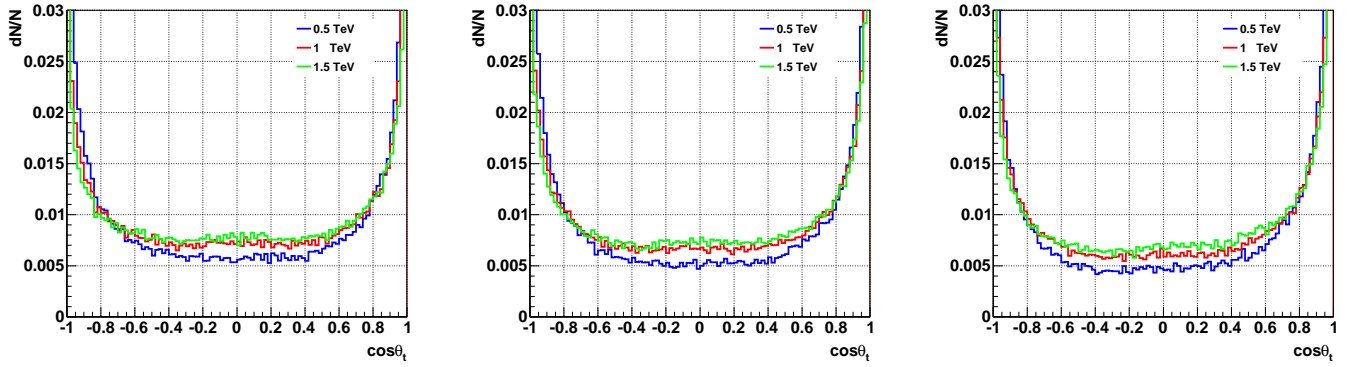


FIG. 9: Angular distribution of the top in tt CM frame with $\sqrt{S} = 7, 10$ and 14 TeV.

using polarized tops, a right handed Z' can be distinguished from the left-handed for at least up to Z' mass of 750 GeV or so.

C. LHC sensitivities to coupling

In order to estimate the LHC sensitivities we assumed that at least 5 same sign dilepton events are observed corresponding to each LHC energy we discussed. In Fig. 10 we plot these for a Z' mass of up to 3 TeV. In the figure, region right to each of the curve is expected to be observed at the LHC besides what is already excluded at the Tevatron [16] as shown in the same Figure. As an example: For one year of LHC run (or equivalently saying, with 10 fb^{-1} data) with $\sqrt{S} = 14$ TeV, the lowest g_X that can be accessed, is $\sim 5 \times 10^{-3}$ which will further improve by a factor $1/\sqrt{\int \mathcal{L} dt}$ as more and more data is collected. One more thing to note that once we include the NNLO-NLL QCD K-factor as given in [7], the lower allowed values of the coupling g_X will go down by a factor of $1/\sqrt{1.2} \sim 1.1$, for a given $m_{Z'}$.

V. RESULTS AND DISCUSSION

We studied same a Z' model that couples to the top quark with flavor off-diagonal coupling in the context of same sign dilepton signatures at the LHC with different LHC energies. We also estimated ratios of -ve signed dilepton with +ve signed dileptons as found that these can serve as an important tool in accessing the Z' mass. We also reconstructed top mass using two techniques namely, through the on-shell mass relation method and the M_{T_2} -Assisted On-Shell (MAOS) Momentum technique and have shown that angular distributions of tops can be helpful in finding the nature of the exchanged Z' .

In the previous subsection, we also estimated LHC sensitivities to coupling with different LHC energies for $m_{Z'}$ up to 3 TeV. Our results show that for an integrated

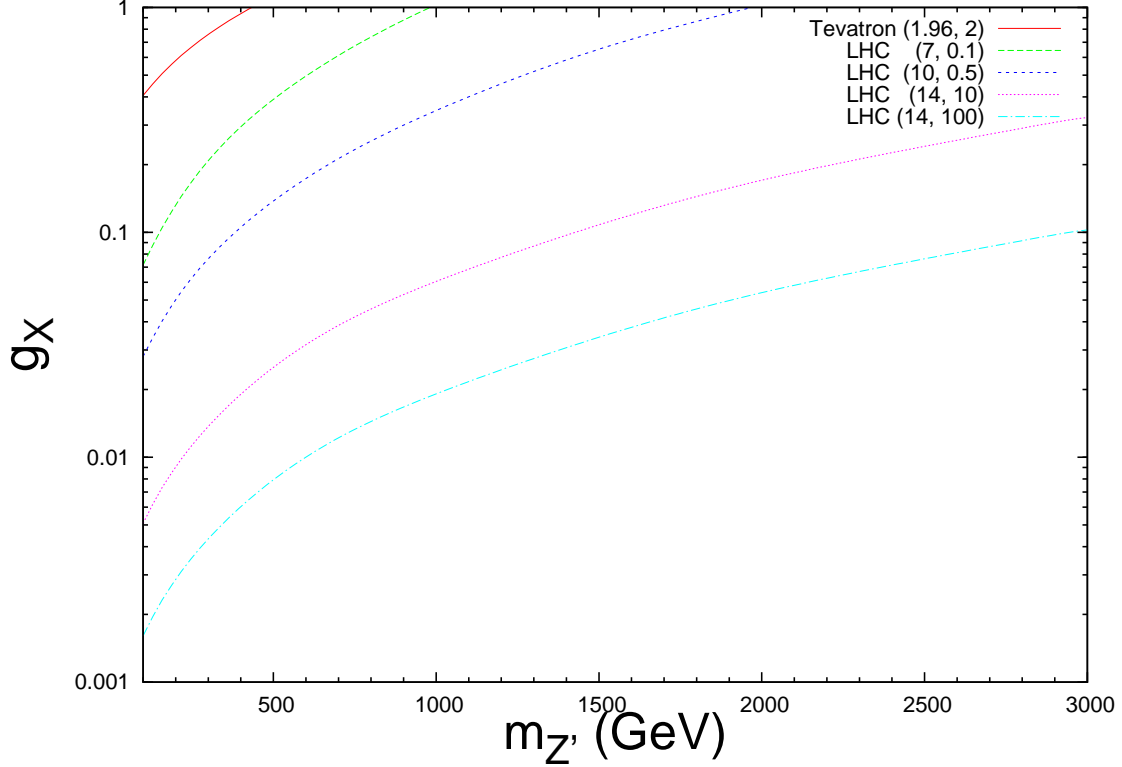


FIG. 10: Allowed $g_X - m_{Z'}$ parameter space at the LHC and Tevatron in same-sign dilepton signal. In brackets are the Centre-of-mass energies (TeV) and integrated luminosities (fb^{-1}) respectively. Region right to each curve corresponds to at least 5 events for the given luminosities.

luminosity of about $\int \mathcal{L} dt = 10 fb^{-1}$, the lowest coupling that can be reached using this signal is $\sim 5 \times 10^{-3}$ or so.

Further studies to measure top polarization [17] and various angular correlations [18] between the final states can be of paramount importance to understand nature of such Z' and its coupling to the quarks.

Acknowledgments

SKG thanks German Valencia and David Atwood for useful discussion and comments, Nils Krumnack and Aranzazu Ruiz Martinez for some help with the ROOT package [19]. The work was supported in part by DOE under contract number DE-FG02-01ER41155.

[1] For a recent review see P. Langacker, Rev. Mod. Phys. **81**, 1199 (2008) [arXiv:0801.1345 [hep-ph]].

- [2] A. Arhrib, K. Cheung, C. W. Chiang and T. C. Yuan, Phys. Rev. D **73**, 075015 (2006) [arXiv:hep-ph/0602175]; X. G. He and G. Valencia, Phys. Lett. B **680**, 72 (2009) [arXiv:0907.4034 [hep-ph]]; O. Cakir, I. T. Cakir, A. Senol and T. Tasci, arXiv:1003.3156 [hep-ph].
- [3] S. K. Gupta, G. Valencia, Phys. Rev. **D82**, 035017 (2010). [arXiv:1005.4578 [hep-ph]].
- [4] S. Jung, H. Murayama, A. Pierce and J. D. Wells, Phys. Rev. D **81**, 015004 (2010) [arXiv:0907.4112 [hep-ph]].
- [5] S. Bar-Shalom and A. Rajaraman, Phys. Rev. D **77**, 095011 (2008) [arXiv:0711.3193 [hep-ph]].
- [6] P. Langacker and M. Plumacher, Phys. Rev. D **62**, 013006 (2000) [arXiv:hep-ph/0001204]; X. G. M. He and G. Valencia, Phys. Rev. D **70**, 053003 (2004) [arXiv:hep-ph/0404229]; X. G. He and G. Valencia, Phys. Rev. D **74**, 013011 (2006) [arXiv:hep-ph/0605202]; C. W. Chiang, N. G. Deshpande and J. Jiang, JHEP **0608**, 075 (2006) [arXiv:hep-ph/0606122]; S. Baek, J. H. Jeon and C. S. Kim, Phys. Lett. B **641**, 183 (2006) [arXiv:hep-ph/0607113]; X. G. He and G. Valencia, Phys. Lett. B **651**, 135 (2007) [arXiv:hep-ph/0703270]; S. Baek, J. H. Jeon and C. S. Kim, Phys. Lett. B **664**, 84 (2008) [arXiv:0803.0062 [hep-ph]]; R. Mohanta and A. K. Giri, Phys. Rev. D **79**, 057902 (2009) [arXiv:0812.1842 [hep-ph]]; V. Barger, L. Everett, J. Jiang, P. Langacker, T. Liu and C. Wagner, Phys. Rev. D **80**, 055008 (2009) [arXiv:0902.4507 [hep-ph]]; V. Barger, L. L. Everett, J. Jiang, P. Langacker, T. Liu and C. E. M. Wagner, JHEP **0912**, 048 (2009) [arXiv:0906.3745 [hep-ph]]; L. L. Everett, J. Jiang, P. G. Langacker and T. Liu, arXiv:0911.5349 [hep-ph].
- [7] N. Kidonakis and A. Belyaev, JHEP **0312**, 004 (2003) [arXiv:hep-ph/0310299].
- [8] H. K. Dreiner, M. Guchait and D. P. Roy, Phys. Rev. D **49**, 3270 (1994) [arXiv:hep-ph/9310291]; W. S. Hou and G. L. Lin, Phys. Lett. B **379**, 261 (1996) [arXiv:hep-ph/9510359]; K. T. Matchev and D. M. Pierce, Phys. Rev. D **60**, 075004 (1999) [arXiv:hep-ph/9904282]; F. Larios and F. Penunuri, J. Phys. G **30**, 895 (2004) [arXiv:hep-ph/0311056]; S. Kraml and A. R. Raklev, Phys. Rev. D **73**, 075002 (2006) [arXiv:hep-ph/0512284]; S. Matsumoto, M. M. Nojiri and D. Nomura, Phys. Rev. D **75**, 055006 (2007) [arXiv:hep-ph/0612249]; F. del Aguila and J. A. Aguilar-Saavedra, JHEP **0711**, 072 (2007) [arXiv:0705.4117 [hep-ph]].
- [9] T. Stelzer and W. F. Long, Comput. Phys. Commun. **81**, 357 (1994) [arXiv:hep-ph/9401258].
- [10] J. Alwall *et al.*, JHEP **0709**, 028 (2007) [arXiv:0706.2334 [hep-ph]].
- [11] J. Alwall, P. Artoisenet, S. de Visscher, C. Duhr, R. Frederix, M. Herquet and O. Mattelaer, AIP Conf. Proc. **1078**, 84 (2009) [arXiv:0809.2410 [hep-ph]].
- [12] T. Sjostrand, S. Mrenna and P. Z. Skands, JHEP **0605**, 026 (2006) [arXiv:hep-ph/0603175].
- [13] G. L. Bayatian *et al.* [CMS Collaboration], J. Phys. G **34**, 995 (2007); G. Aad *et al.* [The ATLAS Collaboration], [arXiv:0901.0512 [hep-ex]].
- [14] C. G. Lester and D. J. Summers, “Measuring masses of semiinvisibly decaying particles pair produced at Phys. Lett. B **463**, 99 (1999) [arXiv:hep-ph/9906349]; A. Barr, C. Lester and P. Stephens, J. Phys. G **29**, 2343 (2003) [arXiv:hep-ph/0304226]; C. Lester and A. Barr, JHEP **0712**, 102 (2007) [arXiv:0708.1028 [hep-ph]]; W. S. Cho, K. Choi, Y. G. Kim and C. B. Park, Phys. Rev. Lett. **100**, 171801 (2008) [arXiv:0709.0288 [hep-ph]]; A. J. Barr, B. Gripaios and C. G. Lester, “Weighing

- Wimps with Kinks at Colliders: Invisible Particle Mass JHEP **0802**, 014 (2008) [arXiv:0711.4008 [hep-ph]]; W. S. Cho, K. Choi, Y. G. Kim and C. B. Park, “Measuring superparticle masses at hadron collider using the transverse mass JHEP **0802**, 035 (2008) [arXiv:0711.4526 [hep-ph]]; G. G. Ross and M. Serna, Phys. Lett. B **665**, 212 (2008) [arXiv:0712.0943 [hep-ph]]; A. J. Barr, G. G. Ross and M. Serna, Phys. Rev. D **78**, 056006 (2008) [arXiv:0806.3224 [hep-ph]]; H. C. Cheng and Z. Han, JHEP **0812**, 063 (2008) [arXiv:0810.5178 [hep-ph]].
- [15] R. M. Godbole, K. Rao, S. D. Rindani and R. K. Singh, arXiv:1010.1458 [hep-ph].
- [16] T. Aaltonen *et al.* [CDF Collaboration], Phys. Rev. Lett. **102**, 041801 (2009) [arXiv:0809.4903 [hep-ex]].
- [17] W. Bernreuther, J. P. Ma and T. Schroder, Phys. Lett. B **297**, 318 (1992); R. Harlander, M. Jezabek, J. H. Kuhn and T. Teubner, Phys. Lett. B **346**, 137 (1995) [arXiv:hep-ph/9411395]; R. M. Godbole, S. D. Rindani, K. Rao and R. K. Singh, AIP Conf. Proc. **1200**, 682 (2010) [arXiv:0911.3622 [hep-ph]]; S. Gopalakrishna, T. Han, I. Lewis, Z. g. Si and Y. F. Zhou, arXiv:1008.3508 [hep-ph].
- [18] W. Bernreuther, O. Nachtmann, P. Overmann and T. Schroder, Nucl. Phys. B **388**, 53 (1992) [Erratum-ibid. B **406**, 516 (1993)]; G. Mahlon and S. J. Parke, Phys. Rev. D **53**, 4886 (1996) [arXiv:hep-ph/9512264]; B. Grzadkowski and Z. Hioki, Phys. Lett. B **529**, 82 (2002) [arXiv:hep-ph/0112361]; S. Frixione, E. Laenen, P. Motylinski and B. R. Webber, JHEP **0704**, 081 (2007) [arXiv:hep-ph/0702198].
- [19] R. Brun, F. Rademakers, Nucl. Instrum. Meth. **A389**, 81-86 (1997).